Cancer Therapy: Clinical

Clinical Cancer Research

Phase I Trial of Combretastatin A4 Phosphate (CA4P) in Combination with Bevacizumab in Patients with Advanced Cancer

Paul Nathan[1], Martin Zweifel[1], Anwar R. Padhani[2], Dow-Mu Koh[3], Matthew Ng[3], David J. Collins[4], Adrian Harris[5], Craig Carden[3], Jon Smythe[6], Nita Fisher[7], N. Jane Taylor[2], J. James Stirling[2], Shiao-Ping Lu[8], Martin O. Leach[4], Gordon J.S. Rustin[1], and Ian Judson[3]

Abstract

Purpose: The vascular disrupting agent (VDA) combretastatin A4 phosphate (CA4P) induces significant tumor necrosis as a single agent. Preclinical models have shown that the addition of an anti-VEGF antibody to a VDA attenuates the revascularization of the surviving tumor rim and thus significantly increases antitumor activity.

Experimental Design: Patients with advanced solid malignancies received CA4P at 45, 54, or 63 mg/m^2 on day 1, day 8, and then every 14 days. Bevacizumab 10 mg/kg was given on day 8 and at subsequent cycles four hours after CA4P. Functional imaging with dynamic contrast enhanced-MRI (DCE-MRI) was conducted at baseline, after CA4P alone, and after cycle 1 CA4P + bevacizumab.

Results: A total of 63 mg/m^2 CA4P + 10 mg/kg bevacizumab q14 is the recommended phase II dose. A total of 15 patients were enrolled. Dose-limiting toxicities were grade III asymptomatic atrial fibrillation and grade IV liver hemorrhage in a patient with a history of hemorrhage. Most common toxicities were hypertension, headache, lymphopenia, pruritus, and pyrexia. Asymptomatic electrocardiographic changes were seen in five patients. Nine of 14 patients experienced disease stabilization. A patient with ovarian cancer had a CA125 response lasting for more than a year. DCE-MRI showed statistically significant reductions in tumor perfusion/vascular permeability, which reversed after CA4P alone but which were sustained following bevacizumab. Circulating CD34$^+$ and CD133$^+$ bone marrow progenitors increased following CA4P as did VEGF and granulocyte colony-stimulating factor levels.

Conclusions: CA4P in combination with bevacizumab appears safe and well tolerated in this dosing schedule. CA4P induced profound vascular changes, which were maintained by the presence of bevacizumab. *Clin Cancer Res; 18(12); 3428–39. ©2012 AACR.*

Introduction

Tumor vascular disrupting agents (VDA) target the existing vasculature of tumors causing rapid vascular shutdown leading to cell death and central necrosis (1). Combretastatin A4 phosphate (CA4P; fosbretabulin), a tubulin-binding VDA, displays potent and selective toxicity toward tumor vasculature (2, 3). CA4P is currently under investigation in phase II trials for ovarian, lung, and anaplastic thyroid cancer (4–6).

In preclinical models following CA4P administration, revascularization and continued proliferation of a viable tumor rim, due at least in part to systemic mobilization and homing of bone marrow–derived circulating endothelial progenitor cells (CEPC) was observed (7, 8). In a mouse model of melanoma, disruption of the VDA-induced CEPC spike by an antiangiogenic antibody resulted in marked reductions in tumor rim size and blood flow as well as enhanced VDA antitumor activity (8). Combination treatment of CA4P with an anti-VEGF antibody resulted in a significantly greater tumor response and growth delay than that achieved with single-agent treatments of CA4P in a clear cell renal carcinoma tumor model in nude mice (9).

Bevacizumab, a humanized anti-VEGF-A monoclonal antibody, prevents VEGF from interacting with receptors on vascular endothelial cells and thereby inhibits its

Authors' Affiliations: [1]Mount Vernon Cancer Centre; [2]Paul Strickland Scanner Centre, Northwood; [3]Royal Marsden Hospital; [4]CRUK and EPSRC Cancer Imaging Centre, Institute of Cancer Research and Royal Marsden Hospital, Sutton; [5]Oxford Radcliffe Hospitals; [6]NHS Blood and Transplant, Headington; [7]Nuffield Department of Clinical Laboratory Sciences, University of Oxford, Oxford, United Kingdom; and [8]Oxigene Inc., San Francisco, California

Presented in part at the AACR-NCI-EORTC International Conference: Molecular Targets and Cancer Therapeutics, Oct 22–26, 2007, San Francisco, CA; and the 44th Annual Meeting of the American Society of Clinical Oncology (ASCO), May 30–June 3, 2008, Chicago, IL.

Corresponding Author: Paul Nathan, Department of Medical Oncology, Mount Vernon Cancer Centre, Northwood, Middlesex HA6 2RN, United Kingdom. Phone: 44-1923-844-966; Fax: 44-1923-844-840; E-mail: p.nathan@nhs.net

doi: 10.1158/1078-0432.CCR-11-3376

Translational Relevance

This article reports the results of the first clinical trial combining a vascular disrupting agent (VDA) with an antiangiogenic agent. Preclinical observations suggest that after initial VDA-induced collapse of tumor vasculature, systemic mobilization and homing of bone marrow–derived circulating endothelial progenitor cells (CEPC) contribute to revascularization and continued proliferation of a viable tumor rim. Disruption of the VDA-induced CEPC spike by an antiangiogenic antibody resulted in marked reductions in tumor rim size and blood flow as well as enhanced VDA antitumor activity. In this trial, the combination of the VDA combretastatin A4 phosphate (CA4P) with the humanized anti-VEGF-A monoclonal antibody bevacizumab appeared safe and well tolerated. Dynamic contrast enhanced-MRI (DCE-MRI) showed statistically significant reductions in tumor perfusion/vascular permeability, which reversed after CA4P alone but which were sustained following bevacizumab. This trial vindicates the decision to study this combination to limit the rapid revascularization that restricts the antitumor activity of VDAs.

proangiogenic effects (10, 11). Bevacizumab is in clinical use in combination with cytotoxic chemotherapy for metastatic colorectal cancer, non–small cell lung cancer, in combination with IFN-α for renal cell cancer, and as single agent for recurrent glioblastoma multiforme (12).

The aim of this study was to determine pharmacokinetics, safety, and tolerability of CA4P given in combination with bevacizumab, to evaluate the antivascular activity of CA4P alone and in combination with bevacizumab using dynamic contrast enhanced-MRI (DCE-MRI), and to assess the effect on the plasma levels of VEGF and granulocyte colony-stimulating factor (G-CSF), cytokines implicated in the acute mobilization of endothelial progenitor cells by VDAs (13), and on blood levels of CEPC.

Patients and Methods

Patient population

Patients with histopathologically or cytologically confirmed malignant solid tumors that had failed standard therapy or for which no life-prolonging treatment existed were eligible for this study.

Study-specific criteria for exclusion were prior therapy with CA4P or bevacizumab, or other agents which target VEGF or VEGFR signaling such as sorafenib and sunitinib, the presence of central nervous system metastases, a diagnosis of non–small cell lung cancer, history of gastrointestinal perforations, hemoptysis within the last 3 months, proteinuria >1 g/24 h, ≥grade II neuropathy, surgery within 28 days of screening visit, prior radical radiotherapy or evidence of vascular damage from radiotherapy, history of cardiac and peripheral vascular disease, and uncontrolled hypertension.

Patients were recruited from 2 centers in the United Kingdom (clinical trials registration NCT00395434). The study was conducted according to the Declaration of Helsinki. The study was approved by participating hospitals' ethical review boards, and all enrolled patients provided written informed consent.

Study design

This was a 2-center, open-label, single-arm study of CA4P at escalating doses of 45, 54, and 63 mg/m^2 (the recommended phase II dose of CA4P) given over 10 minutes i.v. as a single-agent therapy on day 1 and then once every 14 days in combination with a 90-minute i.v. infusion of bevacizumab at a constant dose of 10 mg/kg beginning on day 8 (cycle 1), up to maximum 8 cycles. A modified Fibonacci design was used. Three subjects were evaluated at each dose level. If a dose-limiting toxicity (DLT) was observed in one subject, the cohort was expanded to 6 subjects. If ≥2 subjects experienced a DLT, the cohort at the preceding level was expanded to 6 subjects. If the maximum tolerated dose (MTD) was not found to be at one of the 3 dose levels under study, no further dose escalation was to be conducted.

Assessments of safety and tolerability

Adverse events were assessed using the National Cancer Institute's Common Terminology Criteria for Adverse Events (CTCAE) version 3.0 (14).

DLT was defined as any of the following occurring through cycle 2 and the 14-day observation period, considered to be related to combination therapy: QTc prolongation ≥500 ms, >grade II ventricular arrhythmia, grade III or IV toxicity (except fatigue/asthenia, nausea and/or vomiting, tumor pain or diarrhea), grade ≥ II neuropathy which does not recover to ≤grade I within 14 days after scheduled retreatment, any grade toxicity requiring patient removal from the study in the judgment of investigators.

Treatment assessment

Tumor assessments by computed tomographic scans were based on Response Evaluation Criteria in Solid Tumors (RECIST; ref. 15) and conducted at baseline, before cycle 4, before cycle 8, and at the final follow-up visit.

Pharmacokinetics

The plasma pharmacokinetics of CA4P and its primary metabolic products combretastatin A4 (CA4) and its glucuronide (CA4G) were evaluated during the single-agent CA4P treatment on day 1 pre-CA4P infusion, 10 minutes, 30 minutes, 1, 2, 4, 6, and 24 hours post-CA4P infusion; and also during cycles 1, 4, and 8 (combination therapy) at the following time points: pre-CA4P infusion, 10 minutes, 30 minutes, 1, 2, 4 hours, using validated computer software (WinNonlin, version 3.2; Pharsight Corporation). The area under the CA4P, CA4, and CA4G plasma concentration versus time curves (AUC) was calculated using the linear trapezoidal method (linear interpolation). The terminal elimination phase of the pharmacokinetic profile was either

automatically determined by the software based on the line of best fit (R^2) or visually identified using at least the final 3 observed concentration values for 8 selected subjects and occasions. The slope of the terminal elimination phase was calculated using log-linear regression using the unweighted concentration data.

Pharmacodynamics

DCE-MRI evaluation of tumor vascular parameters. All subjects underwent DCE-MRI evaluation of tumor vasculature. MRI scans were carried out at baseline (2 scans within 1 week of starting CA4P as a single-agent treatment), 3 hours and 6 days post-CA4P single-agent treatment, 3 hours post-CA4P infusion (1 hour before bevacizumab infusion) during first CA4P/bevacizumab combination treatment and 6 days after first CA4P/bevacizumab combination treatment.

MRI was conducted either on a 1.5T MR Siemens Avanto system or a 1.5T Symphony system (Siemens Medical Systems), using comparable imaging protocols. Morphologic images using breath-hold gradient echo T1-weighted and turbo-spin echo T2-weighted sequences were acquired initially. Diffusion weighted (DW)-MRI scans were followed by intrinsic susceptibility weighted T2 scans and T1-weighted relaxivity-based DCE-MRI scans were done in sequence. Full results of the DW-MRI measurements have been published (16) and are not detailed in this report.

1.5T MR Siemens Avanto system: for DCE-MRI, intermediate density-weighted 3-dimensional (3D) gradient-recalled echo (VIBE) sequence images were acquired first (TE = 1.34 ms, TR = 4.36 ms, flip angle = 2 degrees, 12 slices of 5-mm thickness, FOV = 350 mm, acquisition matrix 128^2 and reconstruction matrix 256^2). T1-weighted 3D VIBE sequence images (identical parameters and slice positions as above except flip angle 24 degrees) were then obtained sequentially with a time resolution of 12 seconds (40 time points over 8 minutes).

1.5T Symphony system: for DCE-MRI, intermediate density-weighted 3D gradient-recalled echo (VIBE) sequence images were acquired first (TE = 1.45 ms, TR = 4.36 ms, flip angle = 2 degrees, 12 slices of 5 mm thickness, FOV = 350 mm, acquisition matrix 128^2 and reconstruction matrix 256^2). T1-weighted 3D VIBE sequence images (identical parameters and slice positions as above except flip angle 24 degrees) were then obtained sequentially with a time resolution of 12 seconds (40 time points over 8 minutes).

A bolus of 0.1 mmol/kg body weight of gadopentetate dimeglumine (Gd-DTPA, Magnevist; Bayer) contrast agent was administered at 4 ml/s during the fifth image acquisition (i.e., beginning after 48 seconds) using a power injector, followed by a 20 mL bolus of normal saline at the same rate.

Image and data analysis

Voxel-based calculations were conducted using Magnetic Resonance Imaging Workbench (MRIW) v. 4.2.1, a customized analysis software package developed at the Institute of Cancer Research, London, United Kingdom (17).

A target lesion was identified in each patient, avoiding areas that were prone to artifact (e.g., subcardiac region in the left lobe of the liver or adjacent to the air-filled stomach or colon). For each axial image section, a region of interest (ROI) was drawn free-hand just within the inner border of the target lesion on the baseline T1-weighted image. The process was repeated for all axial image sections that contained the target lesion, although the most cranial and caudal axial sections were excluded to avoid partial volume effects and artefacts from wraparound and excitation profile effects.

Signal intensity enhancement on the T1-weighted DCE-MRI images were assessed quantitatively using the Tofts pharmacokinetic model. Quantitative kinetic parameters were derived from mathematically fitted concentration–time curves (18). A pooled arterial input function (modified Fritz-Hansen) was used for these analyses (19, 20). Derived modeling parameters included the $IAUGC_{60}$ (initial area under the gadolinium concentration–time curve), calculated over the first 60 seconds from the onset of signal intensity increase following injection of contrast (units: mmol s), the volume transfer constant of the contrast agent [K^{trans}—formally called the volume transfer constant between blood plasma and extravascular extracellular space (EES); unit: min^{-1}], leakage space (v_e, units: %), and rate constant (k_{ep}, units: min^{-1}).

Multiecho gradient-echo imaging was carried out and the T_2^* relaxivity (signal intensity decay constant) calculated voxel-by-voxel for regions of interest on each slice. (For each voxel, $\log_n$ (SI) is plotted against echo time TE, then a linear regression is carried out on the data: the gradient of the regression line is $-R_2^*$, the T_2^* relaxivity [unit: s^{-1}].) Data for every scan and for each ROI at a given time point were output as text files, concatenated using MS excel, and statistical variables (mean, median) calculated (21).

Reproducibility analysis

We applied Bland–Altman analysis to evaluate measurement reproducibility of the median of the different MRI parameters calculated on a voxel-by-voxel basis (22) according to the methods of Galbraith and colleagues (23). The differences in the paired baseline MRI parameters for the target lesions were normally distributed (D'Angustino–Pearson test, $P > 0.05$). For Bland–Altman analysis, the differences in the 2 baseline T1-weighted MRI measurements were compared with the averaged baseline MRI parameter values, which were used to derive the within-patient coefficient of variance (wCV), the coefficient of repeatability (r), and the group confidence interval (CI; ref. 16). For comparison of cycle 1, 3 hours, and cycle 1 day 6 MRI data (i.e., after the second infusion of CA4P), the MRI data of the single day 6 measurement (i.e., after the first infusion of CA4P) served as a the new baseline data, using the wCV calculated on the basis of the 2 initial baseline measurements (i.e., before the first infusion of CA4P).

In addition, tumors were analyzed voxel wise to display changes in MRI parameters with drug treatment by color maps. Individual voxels on the center slice of each tumor

were color coded on the basis of the values of the different MRI parameters evaluated.

Cytokine and CEPCs quantification

Exploratory analyses were conducted to assess effects of CA4P alone and in combination with bevacizumab on plasma concentrations of the cytokines VEGF and G-CSF, and blood levels of circulating endothelial cells (CEC), CEPCs, and $CD34^+$ or $CD133^+$ bone marrow–derived progenitor cells. Analyses were conducted before first CA4P administration (day 1); at 4 hours, 24 hours, and 6 days post-CA4P administration; before first CA4P/bevacizumab administration (cycle 1); at 4 hours post-CA4P dose before bevacizumab administration, 24 hours 6 days, or 14 days, respectively, post-CA4P/bevacizumab administration.

VEGF and G-CSF levels in blood plasma (EDTA) were measured by sandwich ELISA (VEGF catalog no. DVE00, G-CSF catalog no. HSCS0B, R&D systems Inc.) and concentrations expressed as pg/mL. CEC, CEPC, and $CD34^+$ or $CD133^+$ progenitor cell populations were quantified by flow cytometry with a BD LSRII machine (Becton Dickinson). CEC were defined as $CD45^-$/dim, $CD34^+$, $CD144^+$, and $CD146^+$. CEPC were defined as $CD45^-$/dim, $CD133^+$, $CD144^+$, and VEGF-$R2^+$. A larger population of mainly hemopoietic progenitor cells were measured with just the $CD45^-$/dim and $CD34^+$ or $CD133^+$ markers. The more defined CEC and CEPC populations would be expected to form only a small proportion of these latter 2 populations. The target cell populations were quantified by numbers gated in relation to the total mononuclear cell gate and this was then cross referenced to the mononuclear cell concentration in the original blood sample as determined by a hematology analyzer (Sysmex SE2100; Sysmex UK Ltd.).

Statistical analysis

One-way ANOVA with and without the Dunnett adjustment, paired *t* test, and simple regression were applied to determine statistical significance of blood pressure (BP) changes. The Wilcoxon signed rank test was used to calculate the statistical significance of changes in cytokine plasma and $CD34^+$ and $C133^+$ blood cell concentrations.

Results

Patient characteristics and dose escalation

A total of 15 patients with a median age of 51 years were enrolled. Patient characteristics are listed in Table 1. Three patients were treated in the CA4P 45 mg/m^2 cohort, 4 in the 45 mg/m^2, and 8 in the 63 mg/m^2 cohort.

Dose-limiting toxicity

Two CTCAE grade III to IV DLTs were seen. One patient developed transient self-limiting asymptomatic atrial fibrillation after being treated at 54 mg/m^2 CA4P on day 1 and was withdrawn from study. A 28-year-old female patient with metastatic hemangiosarcoma and a previous history of hemorrhage treated in the 63 mg/m^2 cohort experienced grade IV liver hemorrhage the day after her cycle 1 combination treatment 2 weeks after treatment, which resolved after 20 days. The patient was withdrawn from the study.

CA4P dose modifications were conducted in a total of 9 patients (2 at 45 mg/m^2, 3 at 54 mg/m^2, and 6 at 63 mg/m^2) due to toxicity.

Toxicity

Highest grade drug-related toxicities per patient over all cycles are summarized in Table 2.

Overall, hypertension was the most common toxicity. Seventy-three percent (11 patients) experienced grade I or II hypertension. No grade III or IV hypertension was seen. Two patients were already on antihypertensive medication at study inclusion. One patient only was treated with amlodipine for grade I hypertension after CA4P infusion on day 1, when BP rose to 163/113 mm Hg. BP time courses over the cycles and over the first 6 hours of CA4P infusion are shown in Fig. 1. BP profile on day 1 confirmed previously published data showing a maximum increase in BP 1 hour after CA4P administration (24). This acute increase was no greater after the third and subsequent cycles of CA4P when patients had previously been treated with bevacizumab. Both systolic and diastolic BP increased in subsequent cycles once bevacizumab treatment started. From cycle 5 on, differences were no longer statistically significant. The greatest statistically significant increase in mean BP compared with the lowest BP measured before cycle 1 was +13 mm Hg (+10%) systolic and +9 mm Hg (+12%) diastolic, respectively. Only the mean of all individual systolic BP during cycle 2 was significantly increased compared with the mean BP over 6 hours measured during cycle 1 (+7 mm Hg or +5%). The mean of highest individual BP during the 6 hours after CA4P administration was significantly increased during cycle 2 and 3 systolic (+16 mm Hg or +11%), and during cycle 3 diastolic (+9 mm Hg or +10%). Note that if ANOVA with the Dunnett adjustment for repeated measures is used, the differences in mean and highest BP respectively over the cycles are no longer significant. Because the most pronounced increase in maximum BP was seen at cycle 3, the hourly BP measurements of day 1 were compared with those of cycle 3. Although the range of systolic BP at 1 hour was greater at cycle 3 (104–202 vs. 115–176 mm Hg), there were no statistically significant differences between the 2 profiles.

There were no statistically significant correlations between dose and BP changes at any time point during the study.

Asymptomatic transient self-limiting grade I or II electrocardiographic changes (T-wave inversion, ST-elevation, ST-depression, and sinus tachycardia) were seen in 5 (33%) patients with no evidence of myocardial damage.

Two patients had preexisting tumor pain, which did not seem to be worsened by CA4P, as previously described (6, 24). Headaches were experienced by 8 (53%) patients.

Rare but important nonhematologic toxicities included neurologic reactions. Two (13%) patients had grade II tinnitus, 3 (20%) patients had dizziness, and one patient (7%) ataxia grade I, probably related to CA4P.

Table 1. Patient characteristics and response

Patient no.	Dose cohort, mg/m^2	Gender/age	ECOG PS	Tumor type	Tumor site	Tumor diameter,[a] cm	Number of cycles	Best response,[b] (RECIST)	TTP,[b] d	Tumor markers
01-01	45	F/49	0	Ocular melanoma	Liver	4.0	7	SD	57	
02-01	45	F/46	1	Ovarian neuroendocrine carcinoma	Liver	6.3	3	PD	—	CA125 increase
						5.6				
						2.6				
						3.7				
02-02	45	F/62	0	Ovarian papillary adenocarcinoma	Bladder	3.2	11	SD	121	CA125 stable
						2.8				
					Pelvic node	3				
01-02	54	M/56	0	Renal cell carcinoma	Muscle	5.3	0[c]	—	—	
02-03	54	F/61	0	Ovarian serous adenocarcinoma	Pelvic mass	8.7	28	SD	373	CA125 response[d]
02-04	54	M/72	0	Colon adenocarcinoma	Liver	8	5	PD	—	CEA decrease
02-05	54	F/50	0	Colon adenocarcinoma	Liver	7.5	10	SD	105	
01-03	63	F/40	1	Melanoma	Subcutaneous node	4.6	3	PD	—	
01-04	63	F/44	1	Melanoma	Liver	3.4	10	SD	57	
01-05	63	F/51	1	Adenocarcinoma of breast	Axillar node	4.6	7	SD	93	
02-06	63	M/52	1	Adenocarcinoma of rectum	Liver	13.4	1	SD	18	
						11.1				
						3.4				
02-08	63	M/80	1	Colon adenocarcinoma	Liver	5.4	8	SD	56	
02-09	63	F/28	2	Hemangiosarcoma of breast	Ovarian mass	6.9	1	NE	—	
02-10	63	M/60	1	Adenocarcinoma of rectum	Sacral mass	9.2	4	SD	44	
02-12	63	F/63	1	Ovarian serous adenocarcinoma	Liver	4.0	3	PD	—	

Abbreviations: CA125, cancer antigen 125; CEA, carcinoembryonic antigen; ECOG PS, Eastern Cooperative Oncology Group performance score; NE, not evaluable; PD, progressive disease; SD, stable disease; TTP, time to progression.

[a]Tumor diameter was measured by DCE-MRI.

[b]Best response and TTP were determined by computed tomographic scan.

[c]Day 1 treatment only.

[d]According to GCIG criteria.

Table 2. Highest grade toxicity per patient (all cycles)

	CTCAE grade			
Adverse event	**I**	**II**	**III**	**IV**
Anemia	40% (6)	7% (1)	—	—
Neutropenia	—	—	—	—
Thrombocytopenia	—	—	—	—
Lymphopenia	47% (7)	7% (1)	—	—
Hypertension	27% (4)	47% (7)	—	—
Headache	40% (6)	7% (1)	7%(1)	—
Pruritus	33% (5)	13% (2)	—	—
Pyrexia	33% (5)	7% (1)	—	—
Pain	13% (2)	13% (2)	7% (1)	—
Dizziness	13% (2)	7% (1)	—	—
Hemorrhage	7% (1)	—	—	7% (1)
Diarrhea	7% (1)	7% (1)	—	—
Nausea	13% (2)	—	—	—
ST depression	13% (2)	—	—	—
Tremor	13% (2)	—	—	—
Tinnitus	—	13% (2)	—	—
Vomiting	13% (2)	—	—	—
Atrial Fibrillation	—	7% (1)	—	—
ST elevation	—	7% (1)	—	—
Ataxia	7% (1)	—	—	—
Sinus tachycardia	7% (1)	—	—	—
T-wave inversion	7% (1)	—	—	—

Pharmacokinetics

Complete plasma data were available for 15 patients for estimation of pharmacokinetic variables for CA4P on day 1, for 14 patients at cycle 1, for 9 patients at cycle 4, and for 5 patients at cycle 8.

The time of maximal plasma concentration was observed 10 minutes after the end of infusion for C4AP and CA4 and at 10 or 30 minutes for CA4G. Plasma concentrations of CA4P and its metabolites were below the detection limit of the assay (2 ng/mL) in all predose samples, on day 1 and on the following cycles, indicating that CA4P and its metabolites were cleared from the plasma between treatment cycles. CA4P became unquantifiable in all patients at 8 hours, whereas CA4 and CA4G could still be quantified at 24 hours. Increases in CA4 and CA4G concentrations were proportional to the increase in CA4P dose from 45 to 63 mg/m^2. No changes in exposure of CA4P or any of the metabolites after combined administration of CA4P with bevacizumab were observed.

In general, exposure of the CA4 and CA4G metabolites remained comparable with that of day 1 after repeated/bevacizumab-combined CA4P administration. After up to 8 cycles of bevacizumab-combined CA4P administration, maximal plasma concentration and AUC of CA4P were reduced to approximately 40% to 70% of those at day 1.

Response

RECIST. Response data are shown in Table 1. No objective responses were seen. Nine (60%) patients' tumors showed stable disease (SD), 4 patients' (27%) tumors showed progressive disease (PD), and 2 patients' responses were not evaluable because of coming off-trial after day 1 and after 2 weeks, respectively, due to adverse events. The tumor of a 61-year-old patient with ovarian serous adenocarcinoma showed a response according to Gynecologic Cancer InterGroup (GCIG) CA125 criteria (25), lasting for more than a year.

DCE-MRI

Group and individual changes in MRI parameters were calculated. The number of individuals showing statistically

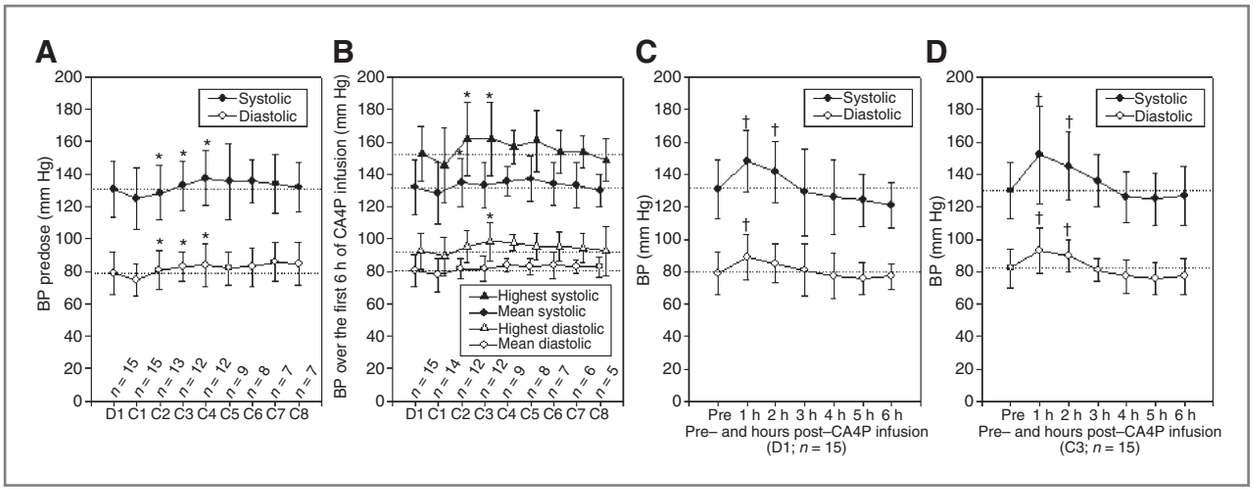

Figure 1. Blood pressure (BP) measurements. BP was measured before the first administration of CA4P on day 1 (D1) and on subsequent cycles (C1–9) before the administration of CA4P and bevacizumab (A). Mean and highest of hourly BP measurements over 6 hours after each administration of CA4P at D1 and over the cycles are shown in B. BP profile over the first 6 hours after CA4P infusion on day 1 are shown in C and on cycle 3 in D. Mean ± SD of the sum of individual measurements are shown. *, $P < 0.05$ (unadjusted) versus cycle 1; †, $P < 0.05$ versus predose.

Table 3. Number of statistically significant individual MRI responses

	Percentage and number of lesions with significant changes[a] (lesions/total evaluable lesions)			
MRI parameter	Three hours after first CA4P (day 1)	Before second CA4P (day 6)	Three hours after second CA4P (cycle 1 day 1)	Six days after second CA4P$^+$ first BV (cycle 1 day 6)
$IAUGC_{60}$	23% (5/22)	11% (2/19)	16% (3/19)	37% (7/19)
K^{trans}	41% (9/22)	11% (2/19)	37% (7/19)	58% (11/19)
v_e	23% (5/22)	5% (1/19)	26% (5/19)	32% (6/19)
k_{ep}	23% (5/22)	13% (2/15)	33% (5/15)	47% (7/15)
R_2^*	30% (7/23)	30% (6/20)	25% (5/20)	26% (5/19)

Abbreviation: BV, bevacizumab.

[a]Change is referred to as decrease for $IAUGC_{60}$, K^{trans}, v_e, and k_{ep}; increase for R_2^*.

significant changes in MRI parameters at 3 hours and 6 days after the first dose of CA4P, and after the second dose of CA4P combined with bevacizumab are shown in Table 3. For 3 patients, more than one lesion was evaluable (see Table 1) and a total of 22 lesions from 15 patients were included in the analysis. No differences in group data analysis were found, whether all lesions from these 3 patients were included in the analysis individually, or if restricted to one concatenated lesion per patient.

The most consistent drug-induced changes were seen in K^{trans}. K^{trans} decreased significantly in 41% of lesions following the first CA4P infusion and recovered at 6 days with 11% of lesions having a significant K^{trans} reduction. Following the second CA4P infusion (but prebevacizumab infusion) 37% of lesions had a significant reduction in K^{trans}. At 6 days, in the presence of bevacizumab, the reduction was maintained with a 58% reduction in K^{trans}. The same trends were seen with $IAUGC_{60}$, k_{ep} and v_e, with reduction and recovery in vascular parameters post-CA4P in a number of lesions and less recovery in the presence of bevacizumab.

In some of the patients with more than one lesion evaluated, there was a high degree of heterogeneity in the response between the lesions. For the intrinsic susceptibility-weighted imaging parameter R_2^*, increases between 25% and 30%, compatible with entrapment of deoxygenated erythrocytes in vasculature, were measured at both time points 3 hours and 6 days after both CA4P or CA4P/bevacizumab combination treatment, respectively.

Group changes in MRI parameters are shown in Fig. 2. A trend toward decreases was seen in both $IAUGC_{60}$ and K^{trans}, whereas v_e and k_{ep} both significantly decreased 3 hours after CA4P infusion, suggesting antivascular effects. This effect was no longer seen 6 days after single-agent CA4P for all 4 parameters, but observed again after the second infusion of CA4P for v_e, k_{ep}, and–albeit not significantly–for $IAUGC_{60}$ and K^{trans}. Combination therapy with CA4P and bevacizumab resulted in a significant and maintained decrease of all 4 DCE-MRI parameters at 6 days, suggestive of a sustained antivascular effect. Intrinsic susceptibility-weighted imaging showed significant increases in R_2^* at all time points after CA4P or CA4P/bevacizumab infusion, suggestive of increased intravascular entrapment of deoxygenated erythrocytes. This effect was more pronounced during the first treatment with CA4P alone.

K^{trans} maps of a pelvic mass in a 61-year-old patient with serous ovarian adenocarcinoma are shown in Fig. 2F.

Cytokine and CEPCs quantification

Plasma VEGF concentrations were significantly increased at 4 hours and returned to baseline at 24 hours after the first CA4P alone infusion. Following the second infusion with both CA4P/bevacizumab, circulating VEGF was undetectable due to the neutralizing effect of bevacizumab (Fig. 3A).

Plasma G-CSF concentrations were significantly increased at 24 hours after both the first CA4P infusion and the second CA4P plus bevacizumab infusion. However, the increase in G-CSF plasma concentration was significantly higher at 24 hours after the CA4P plus bevacizumab infusion than after the CA4P alone infusion (Fig. 3B).

The numbers of CEC and CEPC varied across the different time points but all counts were very low. No significant differences were seen for these cell populations. However there were significant changes in the higher concentrations of the more general $CD34^+$ and $CD133^+$ cell populations. The significant increases in $CD34^+$ and $CD133^+$ cells at 4 hours, the significant decreases at 24 hours, and the return to baseline at 6 days were similar after both the first CA4P and the second CA4P plus bevacizumab infusion. However, $CD133^+$ cell numbers were significantly higher before cycle 1, compared with baseline (Fig. 3C and D).

Discussion

This phase I trial is the first mechanistic DCE-MRI study in humans of the combination of a VDA with an antiangiogenic drug.

An overlapping toxicity of CA4P and bevacizumab is hypertension, which was therefore carefully assessed in this combination study. BP changes were surprisingly mild, with statistically significant mean and peak increases in systolic and diastolic BP in the range of 10% during CA4P/

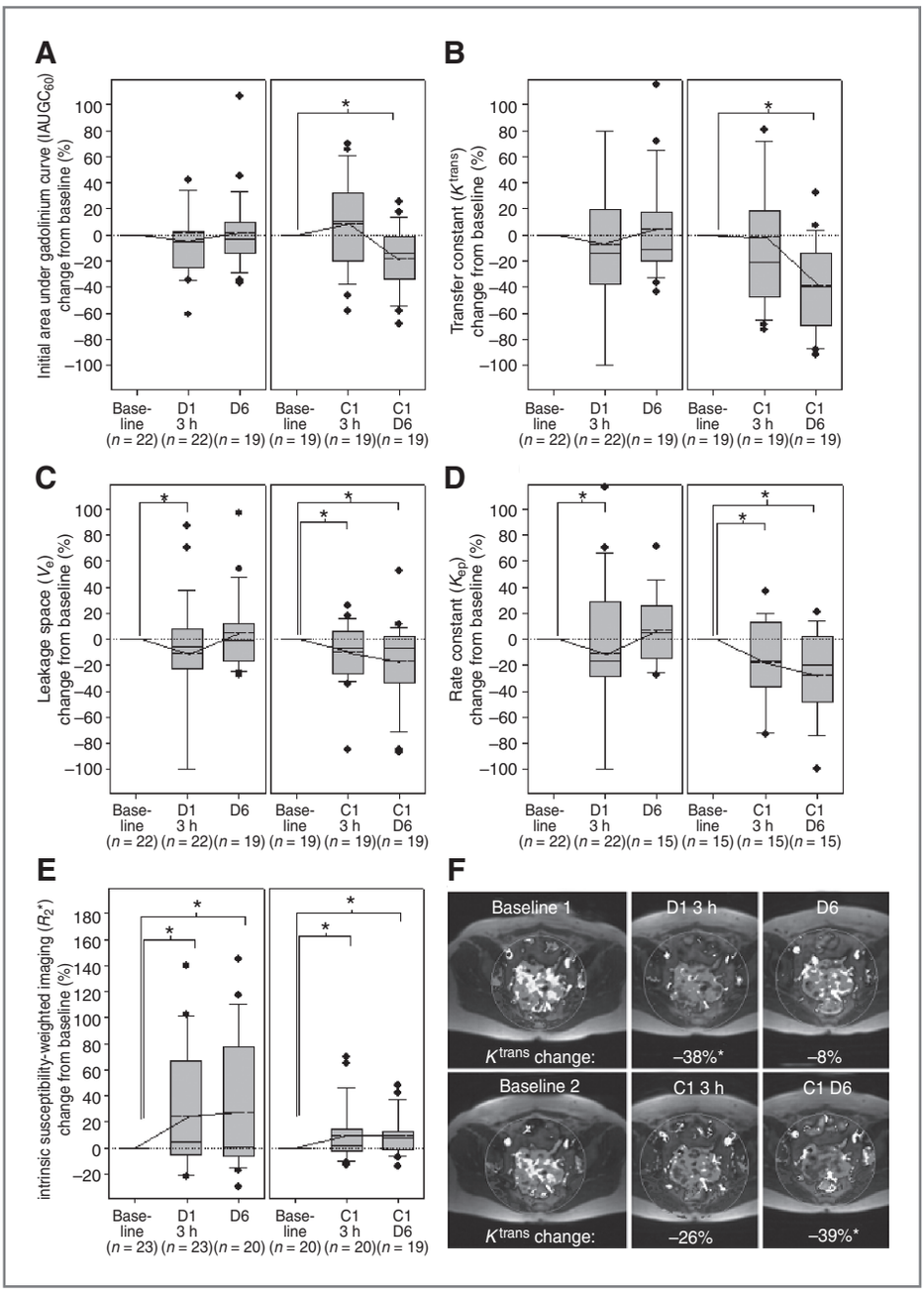

Figure 2. DCE-MRI parameter changes in tumor lesions on day 1 (D1) at 3 hours (3 h) and on day 6 (D6) after the first infusion of CA4P, 3 hours after the second infusion of CA4P on cycle 1 (C1), and on day 6 of combined infusion of CA4P with bevacizumab, respectively. For some patients, more than one lesion was evaluable and included in the analysis. Nonsignificant decreases in $IAUGC_{60}$ by −7% (A) and the transfer constant K^{trans} by −7.3% (B), and significant decreases in leakage space, v_e by 11.2% (C) and rate constant (k_{ep}) by 11.1% (D), 3 hours after the first CA4P infusion, indicating an antivascular effect. This effect is no longer seen 6 days later (+0.7%, +4.7%, +5%, and +7% for the 4 parameters). Similar observations after the second infusion of CA4P for v_e (−9.5%) and k_{ep} (−18.1%), albeit not for $IAUGC_{60}$ (+5.2) and K^{trans} (−1.1%). Adding bevacizumab results in a significant decrease of all 4 parameters (−18.9%, −38.4%, −16.5%, and −28%, respectively) at 6 days, suggestive of a sustained antivascular effect of combination therapy. Intrinsic susceptibility-weighted imaging showed significant increases in R_2^* at all time points after CA4P or CA4P/bevacizumab infusion, suggestive of increased entrapment of deoxygenated erythrocytes (E) within tumors. This effect was more pronounced during the first treatment with CA4P only (+23.9% at 3 hours on day 1 and +27.5% on day 6) than during cycle 1 (+9% at 3 hours and +9.7% at day 6). Failure to reverse R_2^* suggests that erythrocytes are trapped outside vessels. Maps of the DCE-MRI parameter K^{trans}, the volume transfer constant between blood plasma and extravascular extracellular space, in a 61-year-old patient with a pelvic mass of a serous ovarian adenocarcinoma (F). Light tones indicate high K^{trans} values, darker tones indicate lower K^{trans} values. K^{trans} is significantly decreased by 38% at 3 hours after the first CA4P infusion on day 1, but this effect is no longer maintained on day 6, with a nonsignificant K^{trans} decrease of 8.1% compared with the 2 baseline scans. After the second CA4P infusion (cycle 1), a (nonsignificant) K^{trans} decrease of 26.2% is seen again at 3 hours, which becomes even more prominent in combination with bevacizumab at 6 days (39.3%), indicating a sustained antivascular effect. *, $P < 0.05$.

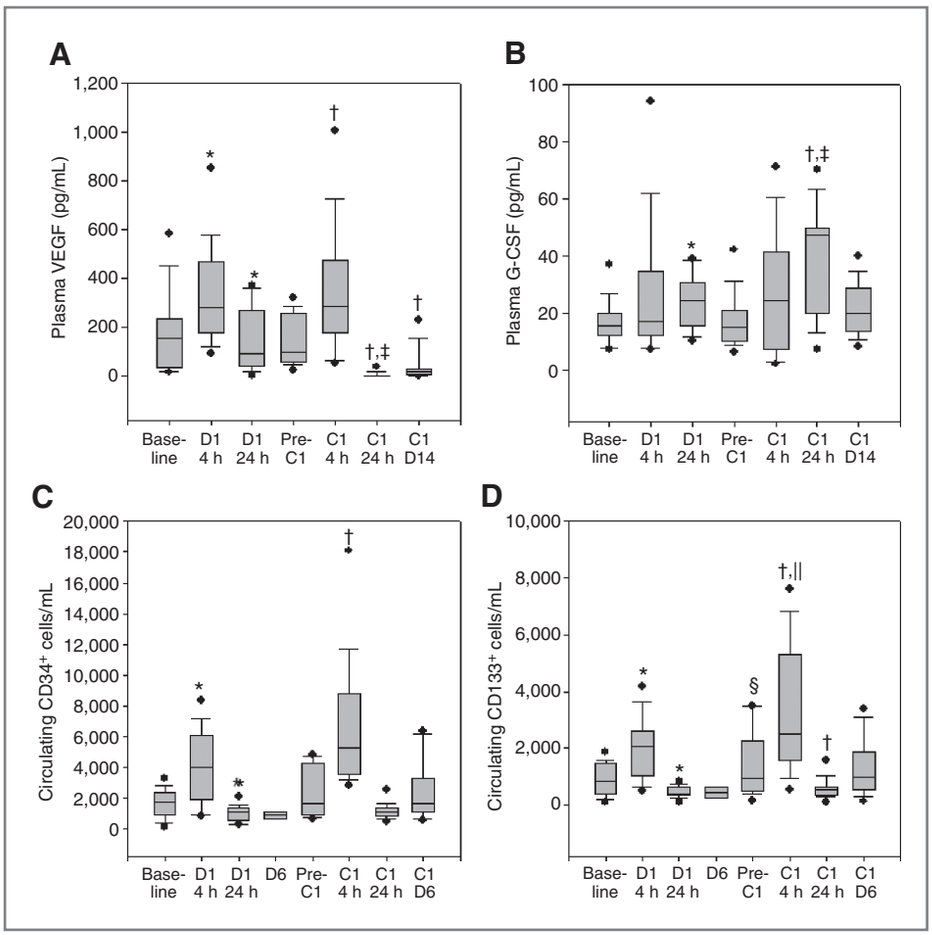

Figure 3. Intraindividual concentrations (unit: pg/mL) of the cytokines VEGF (A) and G-CSF (B) measured in plasma, and circulating $CD34^+$ (C) and $CD133^+$ (D) cells (unit: cells/mL) measured in blood of patients at baseline, on day 1 (D1) at 4 hours (4 h), 24 hours (24 h; A–D), and on day 6 (D6; C and D) after the first infusion of CA4P and before cycle 1 (Pre-C1), cycle 1 (C1) at 4 hours, 24 hours (A–D), and on day 14 (D14; A and B) or day 6 (C and D), respectively, after the second infusion of CA4P combined treatment with bevacizumab. Plasma VEGF concentration is significantly increased at 4 hours, and significantly decreased at 24 hours after both the first CA4P infusion, and the second CA4P/bevacizumab infusion. The decrease in VEGF is sustained at 14 days after CA4P/bevacizumab infusion. However, VEGF concentration is significantly lower at 24 hours after CA4P/bevacizumab infusion than CA4P-only infusion, in keeping with the VEGF scavenging action of bevacizumab (A). Plasma G-CSF concentration is significantly increased at 24 hours after both the first CA4P infusion, and the second CA4P/bevacizumab infusion. However, the increase in G-CSF plasma concentration is significantly higher at 24 hours after CA4P/bevacizumab infusion than CA4P-only infusion, which may be explained by an escape phenomenon of G-CSF due to blocking of VEGF-driven angiogenesis (B). There is no difference between the first CA4P- and the second CA4P/bevacizumab infusion in the significant increases of $CD34^+$ cells at 4 hours, the significant decreases at 24 hours, and the return to baseline at 6 days (C). The significant increases in $CD133^+$ cells at 4 hours, the significant decreases at 24 hours, and the return to baseline at 6 days are similar after both, the first CA4P and the second CA4P/bevacizumab infusion. However, $CD133^+$ cell numbers are significantly higher before the second CA4P/bevacizumab infusion than baseline, and they are significantly increased at 4 hours after CA4P/bevacizumab infusion compared with the first CA4P infusion (D). *, $P < 0.05$ versus baseline; †, $P < 0.05$ versus pre-C1; ‡, $P < 0.05$ versus D1 24 hours; §, $P < 0.05$ versus baseline; and ||, $P < 0.05$ versus D1 4 hours.

bevacizumab combination treatment. There was no evidence of cumulative BP increases during the first 6 hours after CA4P infusion when combined with bevacizumab. The percentage of patients experiencing hypertension was 73%. This is higher than reported for either of the drugs in the literature when used alone (6, 24, 26), but in contrast to previous studies, hypertensive adverse events were all grade I or II only. No patient discontinued on trial because of hypertension.

Well-described side effects of bevacizumab are gastrointestinal perforation, hemorrhage, an increased incidence of arterial thromboembolic complications, and proteinuria (12, 27). In our study, one patient with hemangiosarcoma and a previous history of hemorrhage had grade IV liver hemorrhage, which may have been triggered by either of the study drugs. Neither thromboembolic events nor proteinuria were observed.

There is evidence that after exposure to a VDA, tumor cell repopulation, particularly in the rim of the tumor, may be aided by a reactive systemic host response involving the mobilization of bone marrow–derived circulating cells, including endothelial progenitor cells. These subsequently

home to the vasculature of treated tumors and promote tumor neovascularization. These vasculogenic "rebounds" can be blocked, at least in some preclinical models, by treatment with an antiangiogenic drug (8, 28–30). In our study, DCE-MRI confirmed the increased antivascular activity of CA4P in combination with bevacizumab. Significant decreases in DCE-MRI parameters were seen at 4 hours after the first CA4P infusion but no longer at 6 days. After combination therapy, however, DCE-MRI parameters remained significantly decreased at 6 days, indicating a sustained antivascular effect when CA4P is combined with bevacizumab.

These group changes could be shown despite the marked heterogeneity in individual patient responses to treatment detectable by DCE-MRI, which are to be expected in a phase I study.

R_2^* (BOLD) MRI is a measurement of tumor hypoxia by detection of deoxyhemoglobin. Of interest was the finding that increases in R_2^* signal were maintained following the first exposure to CA4P and did not change with subsequent scans. We interpret this as extravascular sequestration of blood following exposure to the first VDA cycle. Extravascular hemoglobin would remain in place and stay in the deoxygenated form throughout the subsequent scans.

There are only a few trials reporting MRI data of antiangiogenic agents or VDAs combined with chemotherapy. In a trial of preoperative docetaxel with or without bevacizumab for locally advanced breast cancer, Baar and colleagues found a greater decrease in tumor perfusion (calculated by $IAUGC_{90}$) in the combination treatment arm than in the docetaxel-only arm (31).

A more pronounced reduction in K^{trans} (−76%) with bevacizumab in combination with doxorubicin and docetaxel compared with bevacizumab alone (−34%) was found in a trial in inflammatory and locally advanced breast cancer (32). Although no DCE-MRI scan was conducted after day 2, a significant K^{trans} decrease was only seen at the end of cycle 1, but no further decrease at the end of cycle 2 in both arms. A statistically significant decrease in $IAUGC_{90}$ was seen with CA4P, both with and without paclitaxel/carboplatin in a trial of CA4P in advanced malignancies (33). Greater changes were seen in $IAUGC_{90}$ from cycle 1 to 4 than from cycle 4 to 7. This underpins the unique property of CA4P and probably other VDAs eliciting only a short-lived effect on tumor perfusion, further vindicating the need for combining these agents with antiangiogenic agents.

Following CA4P exposure, acute increases in VEGF and G-CSF were observed, mirroring those seen in preclinical models (8). Both VEGF and G-CSF are cytokines implicated in the acute mobilization of endothelial progenitor cells by VDAs (13). In our study, CEC and CEPC numbers were so low (on average less than 50 cells/mL) that these cell populations were not quantifiable with confidence, although the same standardized method detected changes in burns patients (34, 35), patients in a phase I trial of antiangiogenic therapy (36) and patients on OXi4503, another VDA (13, 35). However, the numbers of the overall bone marrow progenitor population $CD45^-$/dim $CD34^+$ or $CD133^+$ cell populations did increase significantly following treatment and the CEC or CEPC populations form a small part of these larger cell populations. These findings concur with preclinical observations (8) that following VDA exposure, bone marrow–derived progenitor cells enter the circulation, populate the tumor, and contribute to angiogenesis.

A number of patients derived significant clinical benefit from treatment even though no RECIST defined responses were seen. A patient with ovarian carcinoma experienced stable disease according to RECIST for more than a year and a CA125 response lasting for more than a year according to GCIG criteria. A heavily pretreated patient with colon carcinoma and a second patient with ovarian carcinoma experienced disease stabilizations for more than 100 days.

The doses recommended for phase II trials must take account of the functional imaging, RECIST, pharmacokinetic, and toxicity data. On the basis of the fact that no pharmacokinetic interaction between CA4P and bevacizumab was found, that toxicity was not dose limiting and the combination generally well tolerated, the recommended doses for phase II trials are 63 mg/m^2 CA4P and 10 mg/kg bevacizumab repeated every 14 days.

In summary, CA4P in combination with bevacizumab appears safe and well tolerated in this dosing schedule with early evidence of clinical activity. CA4P induced an acute increase in circulating bone marrow progenitors, which may in part be mediated by G-CSF and VEGF release. CA4P induced profound vascular changes showed by MRI, which were maintained by the presence of bevacizumab, vindicating the decision to study this combination to limit the rapid revascularization that restricts the antitumor activity of VDAs. This combined approach indicates the way forward in the ongoing clinical evaluation of this novel class of antitumor agents.

Disclosure of Potential Conflicts of Interest

G.J.S. Rustin: advisory board member, OXiGENE, Inc. and Roche. P. Nathan: advisory board member and honoraria from speakers bureau, Roche. No potential conflicts of interest were disclosed by the other authors.

Authors' Contributions

Conception and design: P. Nathan, A.R. Padhani, M. Ng, A.L. Harris, N.J. Taylor, J.J. Stirling, M.O. Leach, G.J. Rustin, I.R. Judson

Development of methodology: P. Nathan, A.R. Padhani, M. Ng, D.J. Collins, A.L. Harris, J.S. Smythe, N. Fisher, N.J. Taylor, J.J. Stirling, M.O. Leach, G.J. Rustin

Acquisition of data (provided animals, acquired and managed patients, provided facilities, etc.): P. Nathan, A.R. Padhani, D.J. Collins, A.L. Harris, C.P. Cardenm, J.S. Smythe, N. Fisher, J.J. Stirling, M.O. Leach, I.R. Judson

Analysis and interpretation of data (e.g., statistical analysis, biostatistics, computational analysis): P. Nathan, M. Zweifel, A.R. Padhani, D.J. Collins, A.L. Harris, C.P. Carden, J.S. Smythe, N. Fisher, N.J. Taylor, J.J. Stirling, S.-P. Lu, M.O. Leach, G.J. Rustin, I.R. Judson

Writing, review, and/or revision of the manuscript: P. Nathan, M. Zweifel, A.R. Padhani, D.-M. Koh, M. Ng, D.J. Collins, A.L. Harris, C.P. Carden, J.S. Smythe, N. Fisher, N.J. Taylor, J.J. Stirling, M.O. Leach, G.J. Rustin, I.R. Judson

Administrative, technical, or material support (i.e., reporting or organizing data, constructing databases): M. Zweifel, D.-M. Koh, D.J. Collins, N. Fisher, N.J. Taylor, J.J. Stirling

Study supervision: P. Nathan, D.-M. Koh, D.J. Collins, J.S. Smythe, M.O. Leach

Acknowledgments

The authors thank the support from Cancer Research UK.

Grant Support

The study was funded in part by OXiGENE Inc., San Francisco, CA. The Drug Development Unit of the Royal Marsden NHS Foundation Trust and The Institute of Cancer Research is supported in part by a program grant from Cancer Research UK. Support was also provided by the Experimental Cancer Medicine Centre (to The Institute of Cancer Research) and the NIH Research Biomedical Research Centre (jointly to the Royal Marsden NHS Foundation Trust and The Institute of Cancer Research).

The costs of publication of this article were defrayed in part by the payment of page charges. This article must therefore be hereby marked *advertisement* in accordance with 18 U.S.C. Section 1734 solely to indicate this fact.

Received January 3, 2012; revised March 1, 2012; accepted March 18, 2012; published OnlineFirst May 29, 2012.

References

1. Patterson DM, Rustin GJS. Vascular damaging agents. Clin Oncol 2007;19:443–56.
2. Pettit GR, Singh SB, Niven ML, Hamel E, Schmidt JM. Isolation, structure, and synthesis of combretastatins A-1 and B-1, potent new inhibitors of microtubule assembly, derived from Combretum caffrum. J Nat Prod 1987;50:119–31.
3. Tozer G, Prise V, Wilson J, Locke R, Vojnovic B, Stratford M, et al. Combretastatin A-4 Phosphate as a tumour vascular-targeting agent: early effects in tumours and normal tissues. Cancer Res 1999;59: 626–34.
4. Study of combretastatin and paclitaxel/carboplatin in the treatment of anaplastic thyroid cancer. Bethesda, MD: NIH; 2011 [cited 2011 Mar 9]. Available from: http://clinicaltrials.gov/ct2/show/NCT00507429.
5. Garon EB, Kabbinavar FF, Neidhart JA, Neidhart JD, Gabrail NY, Oliveira MR, et al. Randomized phase II trial of a tumor vascular disrupting agent fosbretabulin tromethamine (CA4P) with carboplatin (C), paclitaxel (P), and bevacizumab (B) in stage IIIb/IV nonsquamous non-small cell lung cancer (NSCLC): The FALCON trial. J Clin Oncol 28:15s, 2010 (suppl; abstr 7587).
6. Zweifel M, Jayson GC, Reed NS, Osborne R, Hassan B, Ledermann J, et al. Phase II trial of combretastatin A4 phosphate, carboplatin, and paclitaxel in patients with platinum-resistant ovarian cancer. Ann Oncol 2011;22:2036–41.
7. Salmon BA, Siemann DW. Characterizing the tumor response to treatment with combretastatin A4 phosphate. Int J Radiat Oncol Biol Phys 2007;68:211–7.
8. Shaked Y, Ciarrocchi A, Franco M, Lee CR, Man S, Cheung AM, et al. Therapy-induced acute recruitment of circulating endothelial progenitor cells to tumors. Science 2006;313:1785–7.
9. Siemann DW, Shi W. Dual targeting of tumor vasculature: combining Avastin and vascular disrupting agents (CA4P or OXi4503). Anticancer Res 2008;28:2027–31.
10. Marty M, Pivot X. The potential of anti-vascular endothelial growth factor therapy in metastatic breast cancer: clinical experience with anti-angiogenic agents, focusing on bevacizumab. Eur J Cancer 2008;44:912–20.
11. Presta LG, Chen H, O'Connor SJ, Chisholm V, Meng YG, Krummen L, et al. Humanization of an anti-vascular endothelial growth factor monoclonal antibody for the therapy of solid tumors and other disorders. Cancer Res 1997;57:4593–9.
12. U.S. Food and Drug Administration, postmarket drug safety information. Silver Spring, MD: U.S. Food and Drug Administration; 2011 [cited 2011 Mar 9]. Available from: http://www.fda.gov/Drugs/DrugSafety/PostmarketDrugSafetyInformationforPatientsandProviders/ucm193900.htm.
13. Shaked Y, Tang T, Woloszynek J, Daenen LG, Man S, Xu P, et al. Contribution of granulocyte colony-stimulating factor to the acute mobilization of endothelial precursor cells by vascular disrupting agents. Cancer Res 2009;69:7524–8.
14. Common Terminology Criteria for Adverse Events v3.0 (CTCAE). Bethesda, MD: NCI; 2011. [cited 2011 Mar 6]. Available from: http://ctep.cancer.gov/protocoldevelopment/electronic_applications/docs/ctcaev3.pdf.
15. Therasse P, Arbuck SG, Eisenhauer EA, Wanders J, Kaplan RS, Rubinstein L, et al. New guidelines to evaluate the response to treatment in solid tumors. European Organization for Research and Treatment of Cancer, National Cancer Institute of the United States, National Cancer Institute of Canada. J Natl Cancer Inst 2000;92: 205–16.
16. Koh DM, Blackledge M, Collins DJ, Padhani AR, Wallace T, Wilton B, et al. Reproducibility and changes in the apparent diffusion coefficients of solid tumours treated with combretastatin A4 phosphate and bevacizumab in a two-centre phase I clinical trial. Eur Radiol 2009; 19:2728–38.
17. d'Arcy JA, Collins DJ, Padhani AR, Walker-Samuel S, Suckling J, Leach MO. Informatics in Radiology (infoRAD): Magnetic Resonance Imaging Workbench: analysis and visualization of dynamic contrast-enhanced MR imaging data. Radiographics 2006;26:621–32.
18. Tofts P, Brix G, Buckley D, Evelhoch J, Henderson E, Knopp M, et al. Estimating kinetic parameters from dynamic contrast-enhanced T(1)-weighted MRI of a diffusable tracer: standardized quantities and symbols. J Magn Reson Imaging 1999;10:223–32.
19. Fritz-Hansen T, Rostrup E, Larsson HB, L SÍ, Ring P, Henriksen O. Measurement of the arterial concentration of Gd-DTPA using MRI: a step toward quantitative perfusion imaging. Magn Reson Med 1996;36:225–31.
20. Walker-Samuel S, Parker CC, Leach MO, Collins DJ. Reproducibility of reference tissue quantification of dynamic contrast-enhanced data: comparison with a fixed vascular input function. Phys Med Biol 2007;52:75–89.
21. Tofts PS. Modeling tracer kinetics in dynamic Gd-DTPA MR imaging. J Magn Reson Imaging 1997;7:91–101.
22. Bland JM, Altman DG. Measuring agreement in method comparison studies. Stat Methods Med Res 1999;8:135–60.
23. Galbraith S, Lodge M, Taylor N, Rustin G, Bentzen S, Stirling J, et al. Reproducibility of dynamic contrast enhanced MRI in human muscle and tumours-comparison of quantitative and semi-quantitative analysis. NMR Biomed 2002;15:132–42.
24. Rustin GJ, Shreeves G, Nathan PD, Gaya A, Ganesan TS, Wang D, et al. A Phase Ib trial of CA4P (combretastatin A-4 phosphate), carboplatin, and paclitaxel in patients with advanced cancer. Br J Cancer 2010;102:1355–60.
25. Rustin GJ. Use of CA-125 to Assess Response to New Agents in Ovarian Cancer Trials. J Clin Oncol 2003;21:187–93.
26. Rustin GJS, Galbraith SM, Anderson H, Stratford M, Folkes LK, Sena L, et al. Phase I clinical trial of weekly combretastatin A4 phosphate: clinical and pharmacokinetic results. J Clin Oncol 2003; 21:2815–22.
27. Hurwitz H, Fehrenbacher L, Novotny W, Cartwright T, Hainsworth J, Heim W, et al. Bevacizumab plus irinotecan, fluorouracil, and leucovorin for metastatic colorectal cancer. N Engl J Med 2004; 350:2335–42.
28. Shaked Y, Kerbel RS. Antiangiogenic strategies on defense: on the possibility of blocking rebounds by the tumor vasculature after chemotherapy. Cancer Res 2007;67:7055–8.
29. Siemann DW, Rojiani AM. Antitumor efficacy of conventional anticancer drugs is enhanced by the vascular targeting agent ZD6126. Int J Radiat Oncol Biol Phys 2002;54:1512–7.
30. Lyden D, Hattori K, Dias S, Costa C, Blaikie P, Butros L, et al. Impaired recruitment of bone-marrow-derived endothelial and hematopoietic precursor cells blocks tumor angiogenesis and growth. Nat Med 2001;7:1194–201.
31. Baar J, Silverman P, Lyons J, Fu P, Abdul-Karim F, Ziats N, et al. A vasculature-targeting regimen of preoperative docetaxel with or

without bevacizumab for locally advanced breast cancer: impact on angiogenic biomarkers. Clin Cancer Res 2009;15:3583–90.

32. Wedam SB, Low JA, Yang SX, Chow CK, Choyke P, Danforth D, et al. Antiangiogenic and antitumor effects of bevacizumab in patients with inflammatory and locally advanced breast cancer. J Clin Oncol 2006;24:769–77.
33. Akerley WL, Schabel M, Morrell G, Horvath E, Yu M, Johnsson B, et al.A randomized phase 2 trial of combretatstatin A4 phosphate (CA4P) in combination with paclitaxel and carboplatin to evaluate safety and efficacy in subjects with advanced imageable malignancies. Journal of Clinical Oncology, ASCO Annual Meeting Proceedings Part I. Vol 25, No. 18S (June 20 Supplement), 2007: 14060.
34. Fox A, Smythe J, Fisher N, Tyler MP, McGrouther DA, Watt SM, et al. Mobilization of endothelial progenitor cells into the circulation in burned patients. Br J Surg 2008;95:244–51.
35. Smythe J, Fox A, Fisher N, Frith E, Harris AL, Watt SM. Measuring angiogenic cytokines, circulating endothelial cells, and endothelial progenitor cells in peripheral blood and cord blood: VEGF and CXCL12 correlate with the number of circulating endothelial progenitor cells in peripheral blood. Tissue Eng Part C Methods 2008; 14:59–67.
36. Lowndes SA, Adams A, Timms A, Fisher N, Smythe J, Watt SM, et al. Phase I study of copper-binding agent ATN-224 in patients with advanced solid tumors. Clin Cancer Res 2008;14:7526–34.